FEBS Letters

FEBS PRESS
science publishing by scientists

Acid–base chemistry of frustrated water at protein interfaces

Ariel Fernández[1,2]

1 Argentine Institute of Mathematics (I. A. M.), National Research Council (CONICET), Buenos Aires, Argentina
2 Collegium Basilea, Institute for Advanced Study, Basel, Schweiz

Correspondence
A. Fernández, Argentine Institute of Mathematics (I. A. M.), National Research Council (CONICET), Buenos Aires 1083, Argentina
Fax: 54 11 4954 6782
Tel: 54 11 4954 6781
E-mail: ariel@afinnovation.com

(Received 17 September 2015, revised 20 November 2015, accepted 15 December 2015, available online 5 January 2016)

doi:10.1002/1873-3468.12047

Edited by Alfonso Valencia

Water molecules at a protein interface are often frustrated in hydrogen-bonding opportunities due to subnanoscale confinement. As shown, this condition makes them behave as a general base that may titrate side-chain ammonium and guanidinium cations. Frustration-based chemistry is captured by a quantum mechanical treatment of proton transference and shown to remove same-charge uncompensated anticontacts at the interface found in the crystallographic record and in other spectroscopic information on the aqueous interface. Such observations are untenable within classical arguments, as hydronium is a stronger acid than ammonium or guanidinium. Frustration enables a directed Grotthuss mechanism for proton transference stabilizing same-charge anticontacts.

Keywords: anticontacts; hydrogen-bond frustration; interfacial physics; molecular biophysics; protein–water interface; structural biology

Interfacial water enveloping the structure of a soluble protein is often partially confined due to subnanoscale topographic detail in the protein surface [1–3]. When there is a dearth of coordination partners, this confinement brings about frustration of water molecules in regards to their hydrogen-bonding opportunities. Frustration makes water chemically reactive [3], a possibility that needs to be systematically explored. This picture is validated in this work focusing on uncompensated anticontacts or mismatches that classical electrostatics would deem untenable and classical molecular dynamics would treat as unstable. To delineate the frustration-related functionality, we need to focus on the physico-chemical properties of interfacial water that arise from the emergence of interfacial tension, known to be a consequence of frustration [1]. Such properties are not enshrined in a permittivity coefficient stemming from the 'classical' Debye dielectric picture [4]. Due to subnanoscale confinement, the water dipoles are often precluded from aligning with the electrostatic field (**E**), signaling a breakdown in the Debye *ansatz*[4]. This breakdown is marked by the presence of an **E**-orthogonal polarization contribution $\mathbf{P}^{\#}$ that generates a net charge $\gamma^{\#} = -\nabla.\mathbf{P}^{\#}$. The non-Debye term $\mathbf{P}^{\#}$ stores electrostatic energy that may be alternatively computed as interfacial tension [2]. In accord with the charge asymmetry with respect to hydration [5], we provide crystallographic evidence supporting the fact that hydrogen-bond frustration due to nanoscale confinement functionalizes interfacial water as a general base [6], thus determining a *frustration-related chemistry*. The consequences of this chemical role become apparent as we examine conformations featuring same-charge uncompensated anticontacts reported in crystallographic data [7] deemed 'unstable' by classical molecular dynamics (MD) due the absence of nearby counterions. The stabilization of such configurations emerges in a quantum mechanical treatment [3,8], a suitable framework to incorporate frustration-based chemistry. As shown,

Abbreviations
MM, molecular mechanics; MV, mean value theorem; PKMT, protein lysine methyltransferase; QM, quantum mechanical.

the basicity of frustrated water enables titration of ammonium and guanidinium, both weaker acids than hydronium, implying that this effect cannot be accounted for in classical terms. This novel functionality of frustrated water is supported by the crystallographic record and by detailed information on water molecules in intramolecular proton transfer obtained by Fourier Transform Infrared Spectroscopy (FTIR) difference spectroscopy [9]. The results reveal a functionality of biomolecular interfaces intractable by mean-field dielectrics.

Materials and methods

Although Debye polarization accounts for the screening of the solute charge, the $\mathbf{P}^{\#}$-component is responsible for chemical functionality associated with induced charge, hence not accounted for by protein chemical composition. The functionality is in accord with the sign of $\gamma^{\#}$, i. e. proton donor if $\gamma^{\#} > 0$ and proton acceptor if $\gamma^{\#} < 0$. Only one alternative becomes feasible, however. The consequences of such asymmetry will be the object of this study.

To describe the local dielectric distortion of interfacial water, we introduce a 'frustration scalar field' $\phi = \phi(\mathbf{r})$ that quantifies the level of unrealized water hydrogen bonding at spatial location $\mathbf{r}$ relative to the bulk hydrogen-bond pattern [6]. This descriptor is defined as $\phi(\mathbf{r}) = 4 - g(\mathbf{r})$, where $g(\mathbf{r}) \leq 4$ is the time-averaged number of hydrogen bonds (coordination number) that a water molecule sustains whereas it visits a sphere of radius r = 4Å centered at position $\mathbf{r}$ for a minimum time span τ = 1 ns. The choice of temporal and spatial averaging parameters is justified by the need to operate with a smooth scalar field $\phi = \phi(\mathbf{r})$. As expected, the non-Debye field $\mathbf{P}^{\#}$ is proportional to the distortion gradient [6]: $\mathbf{P}^{\#} = -\xi\nabla\phi$, where $\xi = (\lambda\varepsilon_o)^{1/2}$ and λ = 9.0 mJ·m^{-1} at 298K. The net charge $\gamma^{\#}$ induced by $\mathbf{P}^{\#}$ is then $\gamma^{\#} = -\nabla.\mathbf{P}^{\#} = \xi\nabla^2\phi$.

The interfacial energy, $\Delta U_{\phi,}$ associated with spanning the solute–water interface is given by

$$\Delta U_{\phi} = (1/2)\lambda \int ||\nabla\phi||^2 d\mathbf{r}, \quad (1)$$

where integration is carried over a spatial domain Ω containing the interface, so that its border $\partial\Omega$ is fully contained in bulk water, that is, subject to the condition: $\{\phi(\mathbf{r}) = 0 \text{ and } \nabla\phi(\mathbf{r}) = 0\}\ \forall \mathbf{r} \in \partial\Omega$. As the surface integral $\oiint [\phi\nabla\phi].\, d\sigma$ vanishes on $\partial\Omega$, integration by parts yields

$$0 \leq \Delta U_{\phi} = -(1/2)\lambda \int \phi\nabla^2\phi d\mathbf{r} = -(1/2)(\lambda/\varepsilon_o)^{1/2} \int \gamma^{\#}\phi d\mathbf{r} \quad (2)$$

Because $\phi \geq 0$, the mean value theorem (MV) of integral calculus yields:

$$\gamma^{\#}_{MV} = -(\lambda\varepsilon_o)^{-1/2} \int ||\nabla\phi||^2 dr / \int \phi d\mathbf{r} \leq \mathbf{0}, \quad (3)$$

Thus, frustrated interfacial water resulting from nanoscale confinement yields a negative-induced charge $\gamma^{\#}_{MV}$, consistent with a proton-acceptor role resulting from frustrated hydrogen-bond coordination to water oxygen.

This result has important methodological consequences, explaining the acid–base interfacial chemistry explored in the Results section, and may be also obtained based on the hydration differences between positive and negative charges [5]. Such differences arise because the water dipole center differs from the center of its van der Waals sphere, implying that the positive charges on the water protons are closer to the surface of the van der Waals sphere than the negative charge distributed on the lone electron pairs of the oxygen atom. Thus, a solute with negative charge may be more favorably hydrated than one with positive charge as the electrostatic interaction with water protons is facilitated relative to an electrostatic interaction involving the more internalized negative charge in the water molecule. This preferential hydration of negative over positive charges is in accord with the charge asymmetry ($\gamma^{\#}_{MV} \leq 0$, not $\gamma^{\#}_{MV} > 0$) resulting from non-Debye polarization (Eq. 3). A more detailed analysis requires that we consider dehydrons, water-exposed backbone hydrogen bonds that cause subnanoscale confinement and thereby frustration in surrounding water [1–4]. Such dehydrons are primarily hydrated by water molecules interacting with the dehydron carbonyl, rather than the amide (cf. Fig. 1A,B). As the water molecule is presented in the dehydron cavity as a carbonyl solvator, the question remains as to whether it becomes frustrated as proton acceptor (Fig. 1A), by developing a frustration-related negative charge $\gamma^{\#}_{MV} < 0$, or a proton donor ($\gamma^{\#}_{MV} > 0$), with a frustrated dangling hydroxyl (Fig. 1B). The option $\gamma^{\#}_{MV} < 0$ is favored as the negative charge expands due to electronic repulsion within the oxygen shell (Fig. 1A), bringing the charge closer to the water van der Waals surface. This makes it susceptible to better electrostatic interaction with vicinal water protons, located close to the van der Waals surface [5]. This picture has been corroborated in molecular dynamics computations of water-filling dehydron cavities (Fig. 1B, [6]) revealing a negative-induced charge with maximum magnitude 3.31×10^4 Coulomb·mol^{-1} at curvature radius ξ = 2.95 Å.

The presence of nearby dehydrons inducing a proton-accepting role in vicinal interfacial water has been conjectured to enable and steer the intramolecular Grotthuss mechanism of proton transference [8,9]. The free energy change, ΔG, associated with frustration-promoted proton transference is obtained by multiple-steering molecular dynamics computation [10] as described in ref. [3]. The proton donor and nearby proton-receptive water molecule at the dehydron interface are treated within a quantum mechanical (QM) scheme, whereas the rest of the molecule and TIP3P solvent model are treated using a classical molecular mechanics (MM) package, within a QM–MM hybrid approach ([3], Data S1). The dehydron-functionalized water molecule involved in frustration-related chemistry (cf. Fig. 1A) is defined as having its oxygen within 2.5 Å of the

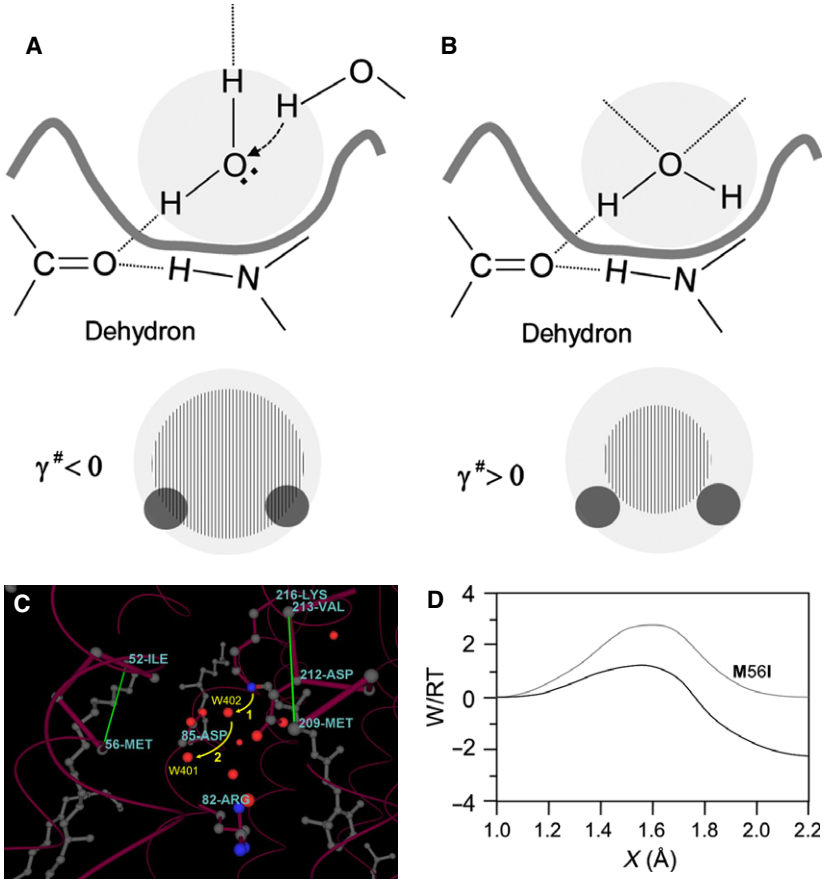

Fig. 1. Protein packing defects, consisting of solvent-exposed intramolecular hydrogen bonds (*dehydrons*), functionalize interfacial water by frustrating water hydrogen-bonding opportunities. (A) Schematic representation of the favored presentation of an interfacial water molecule within the dehydron cavity, featuring a proton-acceptor role resulting from hydrogen-bond frustration due to subnanoscale confinement. The van der Waals sphere is represented in light grey, positive charges are shown in dark grey and the net negative charge ($\gamma^{\#} < 0$) resulting from unsatisfied lone electron pairs within the oxygen orbitals (patterned disk, lower panel) is expanded due to electronic repulsion, approaching the van der Waals border of the water molecule. (B) Disfavored water presentation within the dehydron cavity, yielding $\gamma^{\#} > 0$. The positive polarization-induced charge ($\gamma^{\#} > 0$) favors weaker electrostatic interactions with another water molecule because the latter's negative charge is far from the molecule's van der Waals border when compared with the positive charges on the protons. (C) Dehydron-based water functionalization enables the directed Grotthuss mechanism of intramolecular proton transfer in *bacteriorhodopsin* (PDB 1C3W). The hydronium that results from condensation of K216 and ligand retinal (step **1**) is identified as water molecule W402, whose proton acceptance role is induced by nearby dehydron M209-V213. For simplicity, backbone hydrogen bonds are represented as segments joining α-carbons of paired residues. The transference of this proton to W401 (step **2**) is enabled by the proton-accepting role of water molecule W401, frustrated by the confinement brought about by nearby dehydron I52-M56. Step **2** initiates the directed Grotthuss mechanism. (D) Free energy change $\Delta G(X)/RT = -\log < \exp[-W(X, \mathbf{R}(X))/RT] >$ reported as work (W) in RT units along the pulling coordinate X for the proton transfer Wat402→Wat401 for wild-type (black line) and *in silico* mutant M56I (grey line). The computation is described as noted in main text. The control *in silico* mutant M56I is designed to remove the 52–56 dehydron by increasing the number of nonpolar side-chains in the vicinity the backbone hydrogen bond. As $\Delta G = 0$ for the M56I variant, the proton transference value $\Delta G = -1.41 \pm 0.33$ kcal·mol^{-1} provides a reliable estimation of the effect of dehydron-induced water frustration.

transitional proton that is initially covalently attached to a heavy atom (O, S or N) in the proton-donating moiety, whereas constrained by a distance between backbone carbonyl and water oxygen atoms < 3.3 Å. The proton donor is generically denoted AH (or AH^+, A = O, S, N) and the neighboring distance cut-off is set so that the covalent bond A-H ($[A\text{-}H]^+$ if protonation generates charge) turns into hydrogen bond in the deprotonated state $A{-}H(H_2O)^+$ (or $A{—}H(H_2O)^+$) that results as the proton is transferred to the nearby dehydron-functionalized water molecule.

We denote by X the proton transference coordinate indicating the distance of the proton to the heavy atom A initially covalently attached to it. Thus, $X(t = 0) = X_0$ is the bond length corresponding to covalent bond A-H, and

$X\text{-}X_0$ measures departure from covalent bond length. We denote by **R** the structural-coordinate vector for protein chain and water system. We compute the free energy change as $\Delta G/RT = -\log \langle \exp[-W(X, \mathbf{R}(X))/RT] \rangle$, where the average $\langle \exp[-W(X, \mathbf{R}(X)] \rangle$ (W = computed work) extends over all trajectories $\mathbf{R}(X(t))$ spanned over the time interval $[0, t_f = t_f(v)]$ with conformations steered by the pulling $X = X_0 \rightarrow X = X_0 + v(t_f)$ at constant speed v along the harmonic proton transference linear coordinate during time span t_f [3,10]. The pathway ensemble $\{\mathbf{R}(X(t))\}$, is generated by choosing initial conformations $\mathbf{R_0} = \mathbf{R}(X_0)$ within an isothermal/isobaric equilibrated ensemble (T = 298 K). This ensemble fulfills the condition $X = X_0$ and is generated by a set of 20 classical thermalization trajectories, each lasting 1 ns, with the PDB-reported structure fixed at the initial condition.

We also compute the pKa-shift, ΔpKa, for a proton-donating side-chain group within the protein environment relative to the free residue in solution. The quantity ΔpKa estimates the difference in free energy increment, $\Delta\Delta G/RT = [\Delta G(p) - \Delta G(w)]/RT$, of the proton abstraction process in the protein environment (ΔG(p)) relative to the chemical event taking place in the bulk aqueous environment (ΔG(w)). The free energy computation is performed according to the multiple-steering procedure previously described [3].

Results

The proton-accepting role of interfacial water surrounding dehydrons has been previously conjectured to promote the intramolecular Grotthuss mechanism of proton transference [8,9]. This is clearly not a standard effect of bulk water as the basicity of dehydron-associated water enables titration of ammonium and guanidinium, which are both weaker acids than hydronium. This picture is now validated vis-a-vis detailed information on functional waters in the light-driven proton pump *bacteriorhodopsin* obtained from FTIR difference spectroscopy (PDB 1C3W) [9]. The key role of water molecule Wat401 as initiator of the proton transference cascade is actually enabled by its basicity ($\gamma^{\#}_{MV} = 0.31 \times 10^5$ Coulomb mol^{-1}), in turn conferred by nearby dehydron I52-M56 (Fig. 1C). Hence, the proton in hydronium formed by Wat402, the byproduct of Schiff base condensation between K216 ammonium and the retinal carbonyl, is accepted by Wat401 with $\Delta G = -1.41 \pm 0.33$ kcal·mol^{-1} according to our quantum mechanics computation of dehydron-induced basicity of Wat401. The free energy changes $\Delta G(X)/RT = -\log \langle \exp[-W(X, \mathbf{R}(X))/RT] \rangle$ (black line) are evaluated every 50 ps for pulling speed v = 0.2 Å/ns (Fig. 1D). The average is evaluated over a pathway ensemble $\{\mathbf{R}(X(t))\}$ generated from 20 initial microstates $\mathbf{R_0} = \mathbf{R}(X_0 = 1\text{Å})$ within an isothermal/isobaric equilibrated ensemble (T = 298 K) fulfilling the condition $X = X_0$, with the PDB-reported structure fixed at the initial condition [10]. The results are reported in Fig. 1(D) with the control *in silico* mutant M56I purposely designed to remove the 52–56 dehydron by increasing the number of nonpolar side-chains in the vicinity of residues 52 and 56. As expected, ΔG vanishes for the proton transference from Wat402 to Wat401 in the M56I mutant as no dehydron-associated functionalization occurs (grey line, Fig. 1D). Thus, we can be confident that the proton transference value $\Delta G = -1.41 \pm 0.33$ kcal·mol^{-1} for the wild-type corresponds to the chemical basicity generated by the (I52-M56)-dehydron-induced frustration of Wat401.

An illustration of frustration-related chemistry is provided by the effect of the oncogenic mutation Q790R in Human Epidermal Growth Factor Receptor 3 (HER-3) (ERBB-3) kinase, presumed responsible for recruiting the catalytically active heterodimer HER-3-epidermal growth factor receptor (EGFR) kinase complex [11]. Direct inspection of the interface between mutant HER-3 and EGFR kinase (PDB 4RIX) reveals that the side-chain of R790 in HER-3 is interacting with L668 in EGFR kinase, an unfavorable charged-nonpolar interaction (Fig. 2), treated as anti-

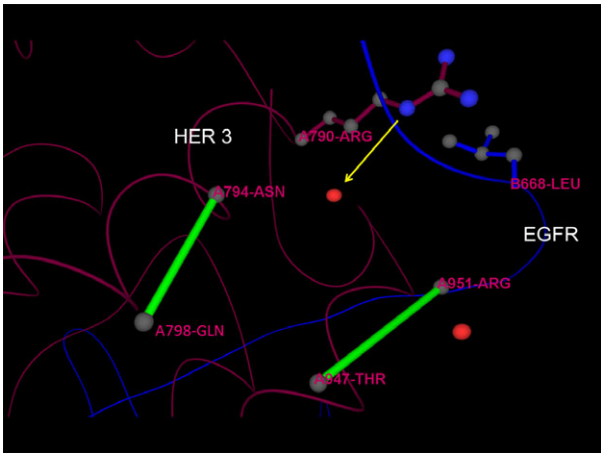

Fig. 2. Role of frustrated interfacial water in the recruitment of the functionally active heterodimer HER3(Q790R)-EGFR (PDB 4RIX, chain A = HER3 Q790R-mutant kinase, chain B = EGFR kinase). The HER3 mutation enables protein association as frustrated interfacial water at dehydron N794-Q798 in chain A accepts the proton from R790 (the arrow marks the chemical event), which is then able to pair favorably with L668 from EGFR kinase at the heterodimer interface, as there is no dehydration cost associated with (neutral-arginine)-leucine pairing. Without invoking frustration-related chemistry, the recruiting effect of mutation Q790R becomes untenable.

contact by classical MD that attributes a positive charge to guanidinium in R790 and a penalty for its hydration hindrance due to proximity to the nonpolar L668. A QM computation, accounting for the frustration-related functionalization of interfacial water vicinal to dehydron N794-Q798, reveals the true recruiting role of the Q790R substitution in HER-3 that, in effect, makes the L668–R790 contact favorable. The recruiting improvement is realized through the deprotonation of R790 promoted by the dehydron-induced basicity of the vicinal water molecule (Fig. 2), with a transference free energy change relative to free arginine in bulk water estimated at $\Delta\Delta G = -2.34 \pm 0.25$ kcal·mol^{-1}.

A more dramatic manifestation of frustration-related chemistry is provided by the L858R oncogenic mutation of the EGFR kinase [12,13], known to promote a more ordered state than the wild-type, thereby lowering the entropic cost of autophosphorylation through homodimerization [14]. Strikingly, the crystal structures of the monomer mutant EGFR kinase (4I20) capture the inactive state with an R836–R858 anticontact (Fig. 3A) which would be deemed as repulsive in classical MD due to a complete absence of

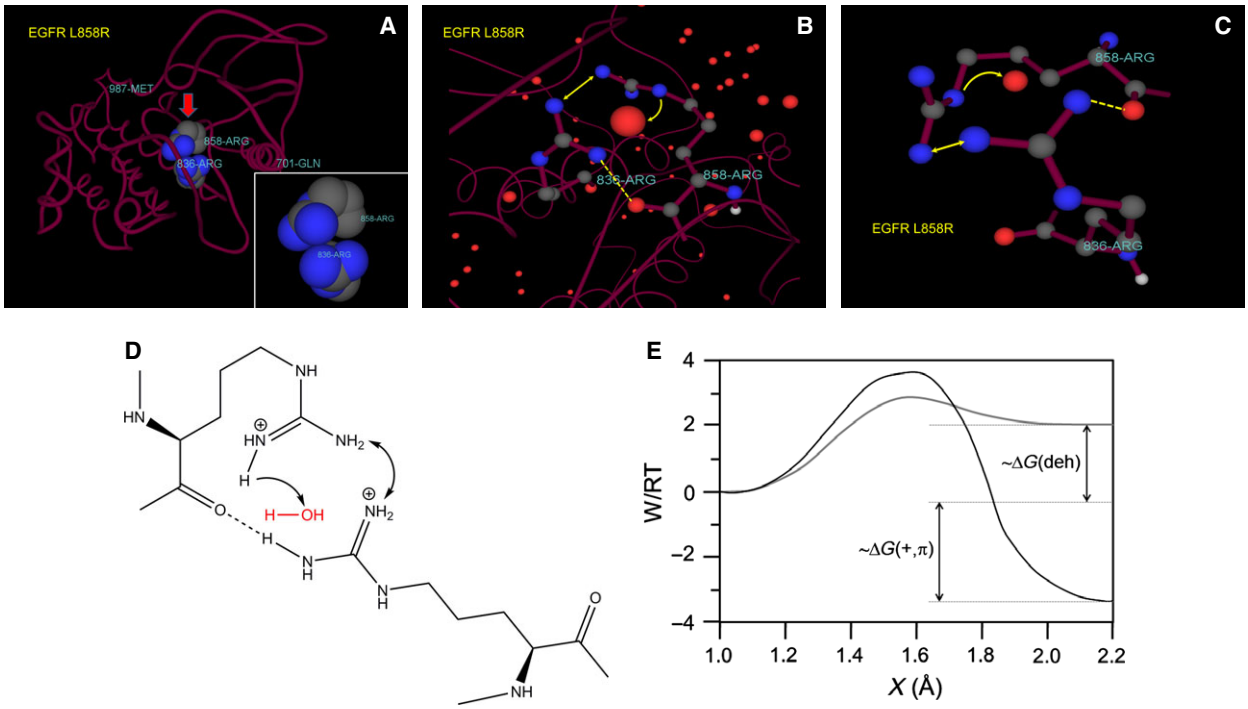

Fig. 3. Frustration-related chemistry of the aqueous interface and its stabilizing role on the classically untenable R836–R858 anticontact in the L858R mutated EGFR kinase (PDB 4I20 and PDB 2ITV). (A) Crystal structure of EGFR mutant reports the mutated residue R858 (signaled by red arrow) making a van der Waals contact with R836 (inset with contact detail). The paired residues are represented at atomic level, while the rest of the chain is featured schematically in tube representation. There is no counterion in the proximity of the association reported in PDB 4I20. The closest negatively charged residues D837, D855, E758 have the carboxyl center farther than 8Å from the (R836, R858) guanidinium centers. None of these residues is engaged in salt bridges with R858, at a variance with the MD analysis in [14]. (B) Quantum effects accounting for frustration-related chemistry of the aqueous interface stabilize the R836–R858 interaction. The R858 guanidinium proton transfers (event marked by arrow) to a water molecule functionalized by the side-chain-main-chain R836–R858 dehydron (dashed line). The proton abstraction from R858 enables a favorable cation-π interaction between protonated R836 and the neutral R858, with its six delocalized π-electrons. (C) Conformation of residues R836 and R858 within the crystal structure of the inactive state (PDB 4I20) featuring the chemically competent side-chain-main-chain dehydron that induces the required basicity needed to remove the electrostatic repulsion between the two vicinal arginines. (D) Frustration-related chemistry enabling the interaction of two arginines through proton transference to a water molecule (water oxygen in red) functionalized by a side-chain-main-chain dehydron. (E) A QM–MM multiple-steering ΔG(X)-computation of the R836–R858-frustrated-water system (black line) contrasted with the control proton transference thermodynamics of guanidine to bulk water (grey line). Computational details are as in Fig. 1(D), and further described in Data S1. The frustrated water molecule (Fig. 3B, C) accepts the proton from the guanidinium in R858 with $\Delta\Delta G = -3.25 \pm 0.27$ kcal·mol^{-1} ($\Delta pKa \approx -5.4 \pm 0.4$). This result yields $\Delta G(+,\pi) = -1.83 \pm 0.18$ kcal·mol^{-1} for the cation-π (836–858)-interaction, since a free energy contribution -1.41 ± 0.33 kcal·mol^{-1} (Fig. 1D) is attributed to the dehydron-induced functionalization of the vicinal water molecule turned into a chemical base.

compensating counterions in the vicinity of the van der Waals contact region (cf. Fig. 3B) [13]. The closest negatively charged residues D837, D855 and E758 all have their carboxyl centers farther than 8Å from the R836, R858 guanidium centers (at the ζ-carbons), in contrast with MD computational models which have them involved in salt bridges with R858 [14]. We rely on the crystal structure information which reveals that the R836–R858 'classical anticontact' prevails and is retained even in the active structure (PDB 2ITV), as shown subsequently.

As expected, classical MD computations report the R836–R858 interaction as unstable and suggest that the oncogenic mutation constitutively deregulates the kinase by destabilizing the inactive state [13]. This interpretation is at odds with the fact that the R836–R858 interaction is sufficiently stable to be captured by the X-ray diffraction patterns of the EGFR kinase mutant and present in all reported structures that are spatial renderings of both the inactive state (PDB 4I20) [12] and of the active state (PDB 2ITV) [15]. The fact that the R836–R858 interaction is found in the crystal structures of inactive and active states of the EGFR kinase mutant suggests that the mutation is not destabilizing the inactive state in the manner modeled by classical MD that computes the van der Waals contact between R836 and R858 as repulsion [13].

As it turns out, the stabilization of the R836–R858 interaction in the inactive state results from a quantum effect with significant decrease in pKa, implicating a water molecule functionalized into basicity by the dehydron sustained by the R836 guanidinium and the backbone carbonyl of R858 (Fig. 3C–E). A QM–MM ΔG(X)-computation of the R836–R858-frustrated-water system (Fig. 3C–E) is contrasted with the control thermodynamics of proton transference of guanidine to bulk water (Fig. 3E), revealing that the frustrated water molecule accepts the proton from the guanidinium in R858 with $\Delta\Delta G = -3.25 \pm 0.27$ kcal·mol^{-1} ($\Delta pKa \approx -5.4 \pm 0.4$). The R858 side-chain deprotonation promotes a favorable cation-π interaction between protonated R836 and the neutral R858, with its six delocalized π-electrons [16]. The results shown in Fig. 3(E) yield $\Delta G(+, \pi) = -1.83 \pm 0.18$ kcal·mol^{-1} for the cation-π (836–858)-interaction. To obtain this estimation, we took into account the contribution of the dehydron-induced water frustration (ΔG (deh)) into ΔΔG, estimated at $\Delta G(deh) = -1.41 \pm 0.33$ kcal·mol^{-1} according to Fig. 1(D), and use the approximate relation: $\Delta\Delta G \approx \Delta G(deh) + \Delta G(+, \pi)$.

The quantum stabilization of this R–R interaction differs significantly from what we may term the 'classical stabilization' achieved through a pair of adjacent counterions. An illustration of the classical R–R stabilization is provided by the homodimer of p53 DNA-binding domain (PDB 2GEQ, Fig. 4A), where the two interacting R178 residues at the dimer interface are compensated by adjacent negatively charged E177 residues pairing two salt bridges (Fig. 4B).

The quantum stabilization of the classically repulsive R836–R858 contact by frustrated interfacial water becomes enhanced in the active state of the EGFR kinase mutant L858R (PDB 2ITV) when this state is compared with the inactive state. In the active state, a favorable interaction between both arginines is enabled by two adjacent side-chain-main-chain dehydrons pairing R858 guanidinium with the backbone carbonyl of R836, and R836 guanidinium with the backbone carbonyl of R858 (Fig. 4C,D). This dehydron pair further enhances the basicity of the vicinal water molecule (Fig. 3C–E), thereby promoting a higher propensity of proton transference ($\Delta\Delta G = -3.75 \pm 0.25$ kcal·mol^{-1}, or $\Delta pKa \approx -6.2 \pm 0.4$) from the R858 guanidinium relative to the inactive state, where only one neighboring dehydron is present (Fig. 3C,D).

The chemical functionality of frustrated water at the protein interface is therefore responsible for the removal of the electrostatic repulsion caused by the special proximity of mutated residue R858 to R836 in the active state of the EGFR kinase. Given that no counterions are found in the vicinity within the crystal structure reported for the inactive state (PDB 4I20), a classical molecular dynamics computation leads to the erroneous conclusion that the repulsion caused by the L858R substitution destabilizes the inactive state, thereby favoring the active state [12]. The main trouble with this argument is that the R836–R858 'anticontact' (distance between ζ–carbons from R836, R858 is 4.28Å) is present in *both* the inactive and the active state. Thus, the assumption arising from MD analysis may be challenged as the inactive conformation reported in PDB actually features a tight van der Waals R836–R858 contact (Fig. 3A) in the absence of counterions (Fig. 3B), which actually persists in time, so as to be captured by X-ray diffraction. Furthermore, this contact, far from being removed, becomes further stabilized in the active conformation (Fig. 4C,D).

In conclusion, at a variance with ref. [14], the R–R interaction in EGFR kinase promoted by mutation L858R is stable in the inactive state. It is not the case that the R836–R858 contact entailing a classical electrostatic repulsion will be disrupted in the inactive state in a conformational exploration ending up in the active state (cf. [13]): the R836–R858 interaction is ***also*** present in the active state (Fig. 4C,D). This interaction

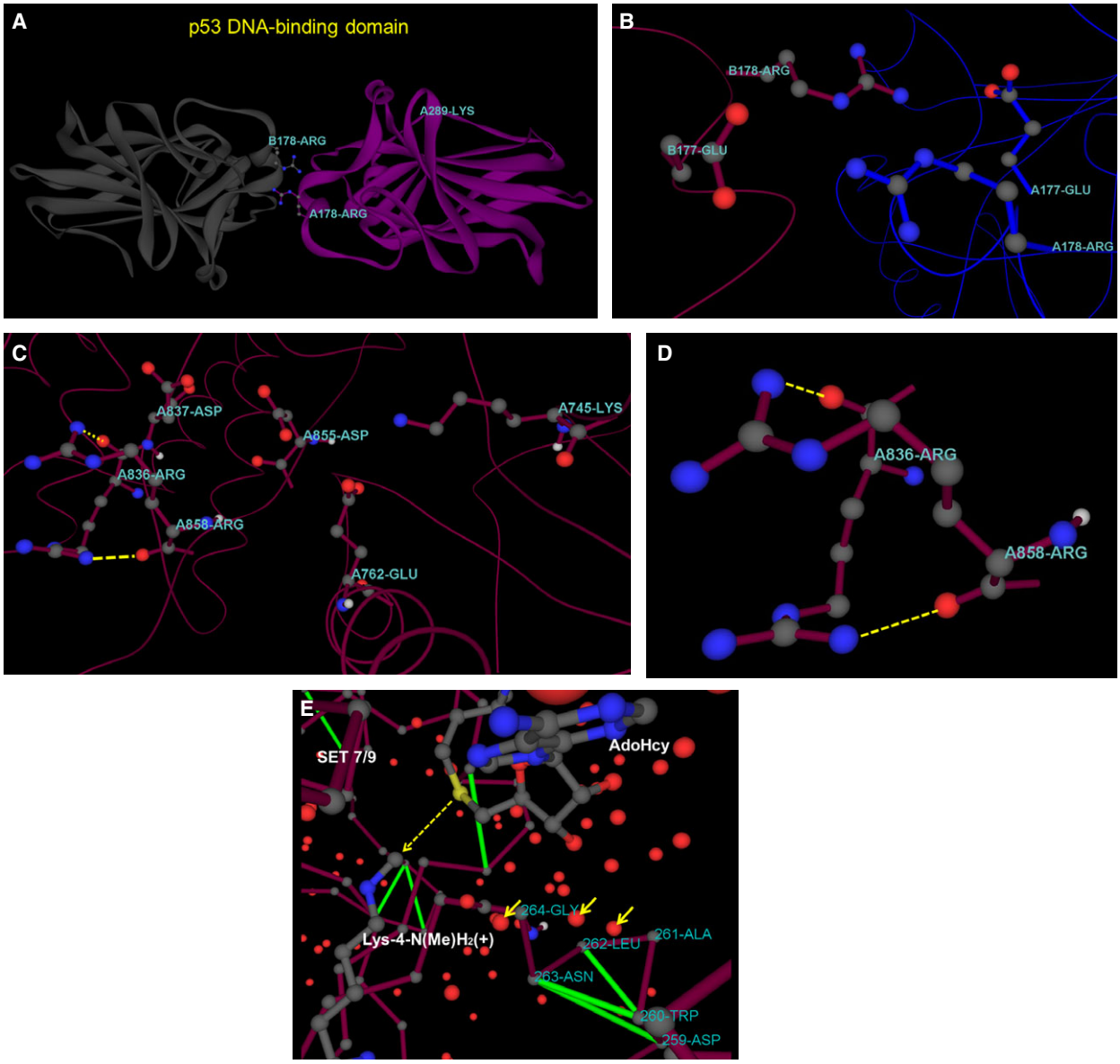

Fig. 4. Illustration of classical electrostatic stabilization of same-charge (R–R) pair (A, B), QM-based stabilization of R–R anticontact (C, D) and of Lys^{+}-$^{+}$AdoMet anticontact within a PKMT complex (E). (A) Functional homodimer of p53-DNA-binding domain displaying the compensated R178-R178 interaction at the protein–protein interface. (B) Detailed structure of R–R association classically stabilized by nearby negative counterions provided by the carboxyls from the twin E177s. (C) Active conformation of EGFR L858R mutant kinase featuring the van der Waals R836–R858 anticontact and the two adjacent main-chain-side-chain dehydrons involving the same interacting residues. These dehydrons confer the aqueous interface the required basicity that removes the electrostatic repulsion between the two adjacent R836–R858 guanidiniums. The closest negatively charged residues D837, D855 and E758 all have their carboxyl centers farther than 8Å from the R836, R858 guanidium centers (at ζ-carbon atoms). (D) Double R836–R858 main-chain-side-chain dehydron stabilizing the R–R side-chain-side-chain interaction in the active structure of the EGFR L858R mutant kinase. (E) Dehydrons (green lines) in PKMT SET7/9 in post-methylation complex (PDB 1O9S) with ligand AdoHcy and methylated substrate Lys-$(Met)H_2^{+}$. Methyl transference is indicated by dashed arrow. The Grotthuss string of dehydron(W260-N263)-functionalized frustrated water molecules (solid arrows) is involved in the proton abstraction from Lys-(NH_3^{+}), a necessary step to enable nucleophilic attack of the neutral Lys amino group on the S-Met bond in $^{+}$AdoMet, yielding Lys-$N(Met)H_2^{+}$.

was never unstable to begin with, even in the complete absence of counterions (Fig. 3B), because the dehydron-promoted interfacial basicity enabled acceptance of the guanidinium proton from Arg858, in turn, enabling a favorable cation-π interaction between protonated R836 and neutral R858. Far from vanishing,

this frustration-related quantum effect is exacerbated in the active state.

The chemistry of interfacial water also plays a key role in enzyme processivity. This assertion is illustrated by the epigenetic mechanism of AdoMet$^+$ (*S*-adenosyl-methionine) methylation of histone(Lys$^+$) catalyzed by a protein lysine methyltransferase (PKMT) [17]. In this context, the histone(Lys$^+$)-$^+$AdoMet anticontact is removed as histone Lys$^+$ becomes deprotonated, which is a necessary step to enable the nucleophilic attack by the (neutral) Lys amino group on the Met-S bond of AdoMet$^+$ [17], yielding epigenetic methylation product Lys(Met)H$_2^+$. The Lys-NH$_3^+$ deprotonation occurs via a directed Grotthuss mechanism within a water channel in the PKMT/substrate/ligand complex [17]. However, *H_3O^+ is a stronger acid than Lys-NH_3^+*, and so *the Grotthuss mechanism can only become feasible if water molecules in the channel are frustrated thereby becoming proton acceptors*. Direct examination of the post-methyl-transfer complex of PKMT SET7/9 with demethylated ligand AdoHcy (*S*-adenosyl-homocysteine) and Lys(Met)H$_2^+$ (PDB 1O9S, Fig. 4E) shows that this is indeed the case. A string of interfacial water molecules (solid arrows in Fig. 4E), beginning with crystal water Wat559, is frustrated due to confinement within the nanocavity of dehydron W260-N263. Thus, a QM computation of frustration-related basicity [3] yields $\Delta\Delta G = -1.65 \pm 0.25$ kcal·mol^{-1}, or $\Delta pKa = 2.7 \pm 0.4$ associated with proton transference from substrate Lys-NH$_3^+$ to the dehydron-functionalized Wat559, in good agreement with other computations [17]. At a variance with the quoted study [17], we note that the decrease in Lys pKa is not the result of same-charge contact within the PKMT complex but of the presence of vicinal frustrated water in the complex, behaving as a general base.

Discussion

We investigated crystal structures reporting uncompensated positive-charge side-chain anticontacts and point mutations generating a positive charge within a pre-existing positively charged environment or within a nonpolar environment. This picture is untenable under the premises of classical electrostatics and prompts a justification of the fact that close positioning of positively charged groups lowers the pKa of the titratable groups [17]. The conundrum is resolved by showing that a crucial chemical feature of interfacial water is missing from the standard analysis. A newly discovered chemical role of interfacial water arising from hydrogen-bond frustration is responsible for the stabilization of classical anticontacts. Thus, the basicity of frustrated water enables titration of ammonium and guanidinium, both weaker acids than hydronium, implying that this effect cannot be captured by a standard approach applicable to bulk water. The appropriate analysis is built upon a quantum mechanical treatment of the proton acceptance event that removes the electrostatic repulsion, causing significant decrease in pKa values relative to the free amino acid in bulk solvent. This frustration-based chemistry is corroborated by the crystallographic record and by detailed spectroscopic information on water molecules in directed Grotthuss mechanisms for proton transfer. Recent PDB-wide bioinformatics data [18] established the anticontact-dehydron motif, upholding the frustration-based chemistry picture put forth in this work.

Acknowledgements

The author is indebted to his former Rice University Ph. D. students Drs. Jianping Chen and Xi Zhang for the implementation of multiple-steering calculations on the Rice Computational Research Cluster. Enlightening conversations with Prof. Ridgway Scott (University of Chicago) are gratefully acknowledged. Support from AF Innovation, a Pharmaceutical Consultancy is acknowledged.

Author contributions

Ariel Fernandez conceived the idea, planned the work, performed the research, generated the data and wrote the paper.

References

1 Fernández A (2012) Epistructural tension promotes protein associations. *Phys Rev Lett* **108**, 188102.
2 Fernández A (2013) The principle of minimal episteric distortion of the water matrix and its steering role in protein folding. *J Chem Phys* **139**, 085101.
3 Fernández A (2015) Packing defects functionalize soluble proteins. *FEBS Lett* **589**, 967–973.
4 Fernández Stigliano A (2013) Breakdown of the Debye polarization ansatz at protein-water interfaces. *J Chem Phys* **138**, 225103.
5 Mobley DL, Barber AE, Fennell CJ and Dill KA (2008) Charge asymmetries in hydration of polar solutes. *J Phys Chem B* **112**, 2405–2414.
6 Fernández A (2014) Communication: chemical functionality of interfacial water enveloping nanoscale structural defects in proteins. *J Chem Phys* **140**, 221102.
7 Magalhaes A, Maigret B, Hoflack J, Gomes JNF and Scheraga HA (1994) Contribution of unusual arginine-

arginine short-range interactions to stabilization and recognition in proteins. *J Protein Chem* **13**, 195–215.
8 Fernández Stigliano A (2015) Biomolecular Interfaces: Interactions, Functions and Drug Design. Springer, Berlin, Epilogue.
9 Garczarek F and Gerwert K (2006) Functional waters in intraprotein proton transfer monitored by FTIR difference spectroscopy. *Nature* **439**, 109–112.
10 Jarzynski C (1997) Nonequilibrium equality for free energy differences. *Phys Rev Lett* **78**, 2690–2693.
11 Littlefield P, Liu L, Mysore V, Shan Y, Shaw DE & Jura N (2014) Structural analysis of the EGFR/HER3 heterodimer reveals the molecular basis for activating HER3 mutations. *Sci Signal* **7**, ra114.
12 Gajiwala KS, Feng J, Ferre R, Ryan K, Brodsky O, Weinrich S, Kath JC and Stewart A (2013) Insights into the aberrant activity of mutant EGFR kinase domain and drug recognition. *Structure* **21**, 209–219.
13 Sutto L and Gervasio FL (2013) Effects of oncogenic mutations on the conformational free-energy landscape of EGFR kinase. *Proc Natl Acad Sci USA* **110**, 10616.
14 Shan Y, Eastwood MP, Zhang X, Kim ET, Arkhipov A, Dror RO, Jumper J, Kuriyan J and Shaw DE (2012) Oncogenic mutations counteract intrinsic disorder in the EGFR kinase and promote receptor dimerization. *Cell* **149**, 860–870.
15 Yun CH, Boggon TJ, Li Y, Woo MS, Greulich H, Meyerson M and Eck MJ (2007) Structures of lung cancer-derived EGFR mutants and inhibitor complexes: mechanism of activation and insights into differential inhibitor sensitivity. *Cancer Cell* **11**, 217–227.
16 Dougherty DA and Ma JC (1997) The cation-π interaction. *Chem Rev* **97**, 1303–1324.
17 Zhang X and Bruice TC (2008) Enzymatic mechanism and product specificity of SET-domain protein lysine methyltransferases. *Proc Natl Acad Sci USA* **105**, 5728–5732.
18 Scott LR & Fernández Stigliano A (2015) Mismatched ions indicate quantum effects in proteins. The University of Chicago, Department of Computer Science Technical Report TR-2015-10.

Supporting information

Additional supporting information may be found in the online version of this article at the publisher's web site:
Data S1. QM/MM Computations.